A different route to functional polyolefins: olefin-carbene copolymerisation

Franssen, N.M.G.; Reek, J.N.H.; de Bruin, B.

DOI
10.1039/c3dt32941k

Publication date
2013

Document Version
Final published version

Published in
Dalton Transactions

Electronic Supplementary Material (ESI) for Dalton Transactions

Supporting Information belonging to the paper:

A different Route to Functional Polyolefins: Olefin-Carbene Copolymerisation

Nicole M. G. Franssen,[a,b] Joost N. H. Reek[a] and Bas de Bruin*[a]

[a] *Van `t Hoff Institute for Molecular Sciences (HIMS), Department of Homogeneous and Supramolecular Catalysis, Universiteit van Amsterdam, P.O. Box 1090 GS Amsterdam, The Netherlands.*
[b] *Dutch Polymer Institute DPI, P.O. Box 902, 5600 AX Eindhoven, The Netherlands.*

E-mail: b.debruin@uva.nl

Contents

Size-exclusion chromatography (SEC) **2**

Kinetics and analysis of minor side products formed **2**

Schematic representation of the various activation processes **3**

^{1}H NMR spectrum of the oligomer fraction **4**

DSC curves of a copolymer sample containing 9% **4**

Computational study concerning branch formation **4**

References in the Supporting Information **9**

Size-exclusion chromatography (SEC)

The copolymer samples obtained with catalysts **1** and **2** reveal a unimodal molecular-weights distribution, with overlapping signals for refractive index (RI) and UV (254 nm) detection over a broad range of M_w (Figure S1, left). This indicates that the homopolymers and copolymers present in the mixture have similar molecular weights, and thus cannot be separated based on their M_w. The copolymers obtained with catalyst **3** reveal a slightly bimodal distribution, with two separate peaks observed close to each other that overlap to some extent (Figure S1, right). Similar patterns are observed for EDA homopolymers obtained with this catalyst, although in that case the splitting pattern is less pronounced.[1]

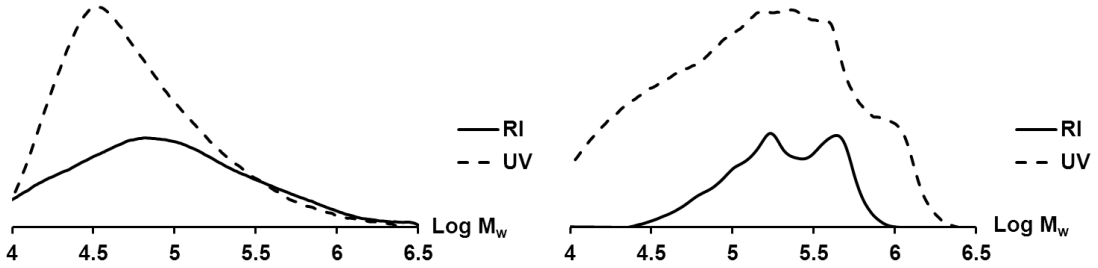

Figure S1. SEC traces of copolymer samples made by catalyst 1 (left) and catalyst 3 (right) showing overlap of refractive index (RI) and UV (254 nm) traces over a broad range of M_w.

Kinetics and analysis of minor side products formed during co-polymerisation

The rates for EDA consumption and polymer formation are somewhat lower in presence of ethene due to competition of EDA and ethene for vacant sites at the metal centre. The formation of oligomers and carbene dimers (diethyl maleate and diethyl fumarate) is mainly observed in the first 10 minutes of reaction after which their content stays constant over time (see Figure S2), and the total content of oligomers in the mixture is slightly lower in presence of ethene. This is in agreement with the proposed different structures of the active species for polymerisation and dimerisation/oligomerisation.[1]

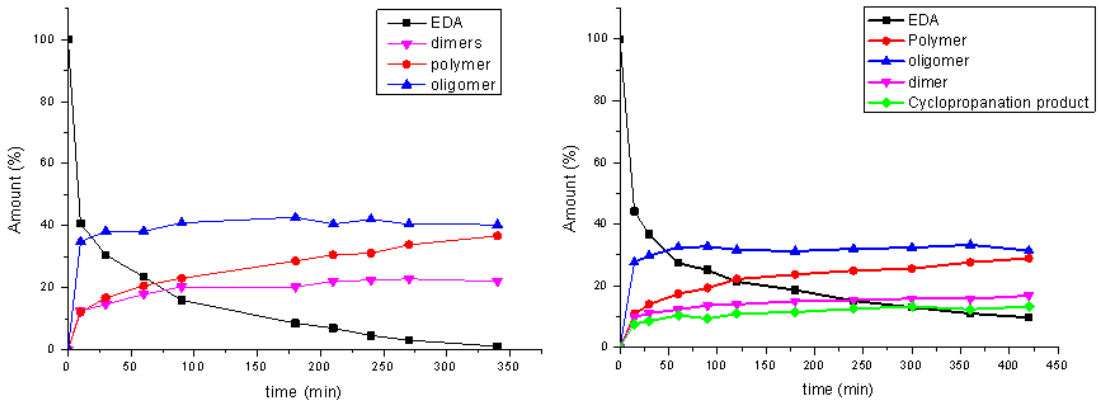

Figure S2. Kinetic profile of the EDA homopolymerisation (left) and ethene-EDA copolymerisation at P_{ethene} = 2 bar (right) catalyzed by complex 1.

Aside from these products, the reaction yields several volatile organic compounds, of which ethyl cyclopropanecarboxylate is the major product (NMR). This product is formed by cyclopropanation of ethene by EDA in about 12% yield. The formation of this product occurs

rapidly during the first 10 minutes of reaction, after which its formation continues at a lower rate. Formation of this product was not enhanced when the reaction was performed at an ethene pressure of 6 bar. Control experiments in which we exposed ethyl cyclopropanecarboxylate to catalyst **1** under similar conditions as used for the polymerisation experiments did not yield polymeric material, thereby excluding participation of this compound in the copolymerisation reactions. Cyclopropanation is efficiently catalysed by dinuclear Rh^{II}-complexes such as $Rh_2(OAc)_4$ and the generally accepted mechanism for this reaction involves concerted carbene transfer from a Rh-carbenoid species to the olefin.[2] Werner and coworkers have shown that cyclopropanation is also feasible from Rh^{I}-carbene complexes, depending on the nature of the ancillary ligands.[3, 4] It could well be that Rh^{I}-carbene species are in our case responsible for the observed formation of ethyl cyclopropanecarboxylate. However, since several Rh species are formed during the catalyst activation process, we cannot rule out participation of a (small amount) of Rh^{II} species in this reaction. Other volatile organic compounds formed duing the reaction of **1** with EDA in an ethene atmosphere are ethyl-2-butanoate and ethyl-3-butanoate, albeit in much smaller quantities (less than 1% of the total product yield). Formation of these compounds is thought to involve formation of an (olefin)Rh^{I}(carbene) complex, in which both ethene and the carbene species are coordinated to the Rh center.[3] From this species, a metallocyclobutane derivative can be generated and this leads to the observed olefinic products via a (π-allyl)Rh(hydrido) intermediate (see Werner *et al.*[3]). A third volatile side product that could be identified was ethyl acrylate, which could possibly be formed in a metathesis reaction (about 2% yield). Due to their volatility, each of these products could be easily removed from the reaction mixture by evaporation.

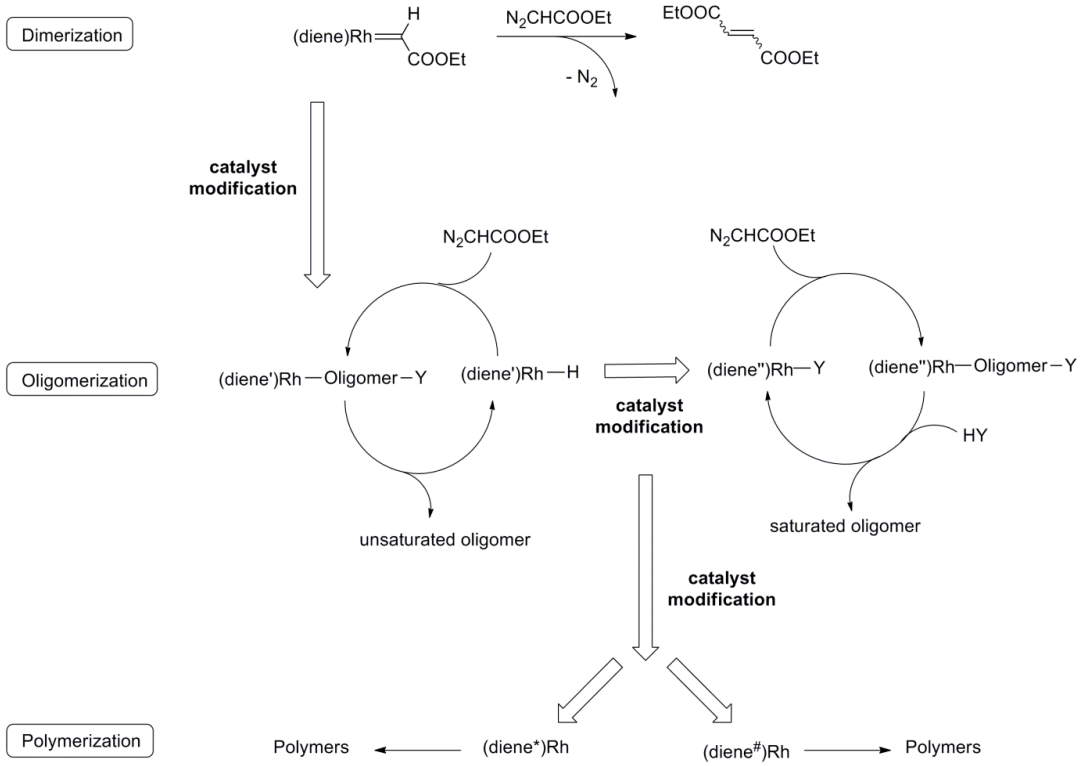

Figure S3. Schematic representation of the various activation processes leading to the formation of the actual active species for polymerisation as observed for Rh^{I}(cod) complexes 1-3.

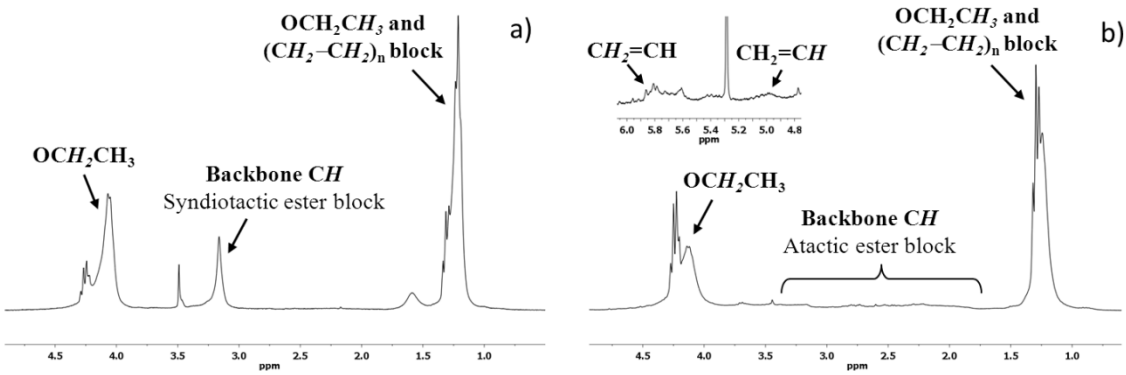

Figure S4. ^{1}H NMR spectrum of the oligomers obtained in the copolymerisation of ethene and EDA catalyzed by complex 1: syndiotactic-rich fraction (a) and atactic fraction (b).

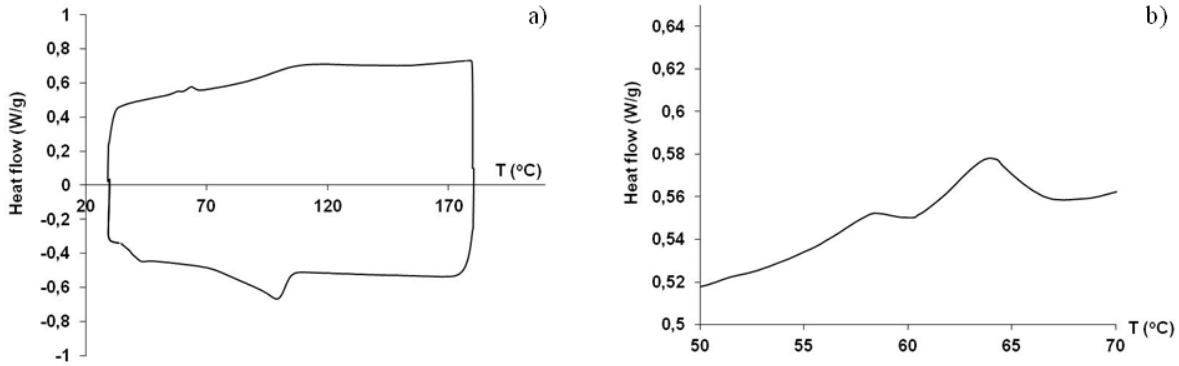

Figure S5. DSC curves of a copolymer sample containing 9% ethene obtained with catalyst 1 (a), and zoom of the region between 50°C and 70°C (b).

Computational study concerning branch formation

As described in the main paper, the copolymers of EDA and ethene are obtained as branched materials, while the EDA homopolymers are highly linear. Similar copolymers obtained in the reaction of EDA with diazomethane (N_2CH_2; leading to insertions of methylene units) are as well obtained as linear materials,[5] and as such the observation of branches for the copolymers described in this paper was rather surprising. To understand the origin of this branch-formation, we performed a computational study.

Previous papers reported by our group point towards involvement of a Rh^{III} species as the active species for carbene polymerisation.[6,7] Most likely, this species is very close in structure to the (allyl)Rh^{III}(alkyl) species **6** as depicted in the main paper. The smallest model system that realistically represents the environment at active species **6** is the cationic $[(allyl)Rh^{III}((CH_2)_3Me)]^+$ (**A'**). This species can be considered to be formed by two consecutive ethene insertions into the Rh–H bond. In order to be able to compare the results of these computations with those described previously concerning the formation of linear copolymers from EDA and diazomethane with the aim to find differences in the branching behaviour, we decided to use the dimethylether-solvated species $[(allyl)Rh^{III}((CH_2)_3Me)(OMe_2)]^+$ (**A**) as analogue of species **A'** as a starting point for our computational studies.

Formation of branches is generally believed to occur after chain termination via β-hydride elimination, leading to the formation of a Rh–H species and an 1-alkene fragment. In a previous publication we already reported that this β-hydride elimination process from species **A** occurs readily at the reaction temperature.[6] The thus generated 1-alkene fragment can participate in subsequent reactions by (re)insertion in either the Rh–H bond generated in the β-hydride elimination step or the Rh–C bond of a growing polymer chain. These possibilities and the resulting products are schematically depicted in Figure S6. Reinsertion of the 1-alkene into the Rh–H bond in a 1,2-fashion leads to the formation of a linear alkyl chain and as such it regenerates Rh-species **A**. Consequently, this pathway does not lead to the formation of branches and will therefore not be considered further. On the other hand, rotation of the 1-alkene followed by insertion into the Rh–H bond in a 2,1-fashion does give rise to branch formation and leads to the formation of product **B**, in which the branch is present at the α-carbon atom of the growing polymer chain. Subsequent insertions of ethene or EDA into the Rh-C bond of **B** will lead to chain extension, giving rise to the formation of branched polymers. However, the energy barrier for ethene insertion into the Rh–C bond of **B** is expected to be much higher than the insertion of ethene in the Rh–C bond of **A**, leading to linear products. Similar results are obtained for insertion of diazomethane in this structure **A**.[6] As such, this pathway would not explain the formation of branches since insertions leading to the formation of linear polymers are clearly favored. Therefore we focused on the possible formation of branches via insertion of 1-alkenes (after dissociation from the Rh center) into the Rh–C bond of complex **A**. To study the viability of this pathway, we compared the energies for this process with those associated with insertion of ethene into this same Rh–C bond, which will be discussed at the bottom of this section.

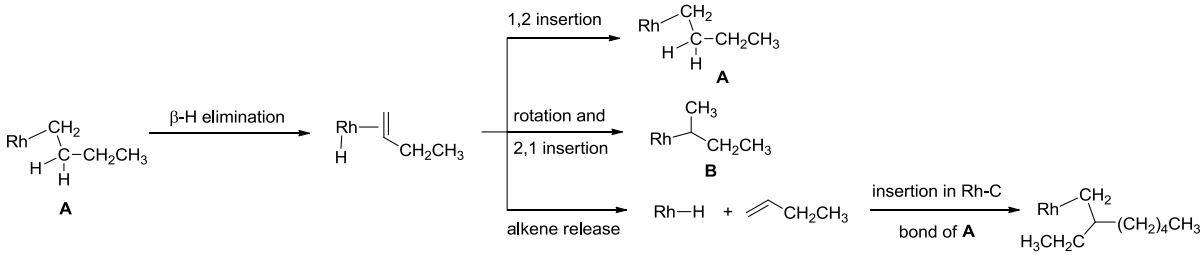

Figure S6. Schematic representation of possible pathways leading to the formation of branches from starting complex A.

We studied the insertion of propene as representative model system for the insertion 1-alkenes into the Rh–C bond as a potential pathway to form alkyl-branched polymers (Figure S7 and Table S1). The results of these calculations have been reported in our previous publication,[6] but are incorporated here for reasons of clarity. Coordination of propene to species **A** is slightly endothermic and leads to the formation of species **C** (+1.2 kcal mol^{-1}). In this species propene is coordinated *trans* to the allyl moiety of the cycloocta-2,5-dien-1-yl ligand. The CH_3 group of the propene moiety is located at the side of the CH_2–CH_2 moiety of the cycloocta-2,5-dien-1-yl ligand but is pointing away from that ligand (Figure S8). Coordination modes in which the methyl fragment of the propene is pointing towards the CH_2 fragment of the cycloocta-2,5-dien-1-yl ligand have a similar energy (**C'** +0.01 kcal mol^{-1}, Figure S9). Coordination of propene with the CH_3 fragment pointing towards the cycloocta-2,5-dien-1-yl ligand, facing either its CH_2 fragment or the CH_2–CH_2 fragment, are slightly higher in energy (**C"** and **C'"** +1.2 kcal mol^{-1}, Figure S9). In these species **C''** and **C'"** the OMe_2 fragment has dissociated from the Rh center, and apparently this dissociation does not

lead to a large increase in energy. The transition state for 1,2-insertion of propene occurs with a free energy barrier of 26.4 kcal mol^{-1} and this transition state is accompanied by a dissociation of the OMe_2 moiety from the Rh center. The release of the OMe_2 fragment has most likely only a small contribution to the total energy barrier, in a similar fashion as observed for species **C** vs. **C''** and **C'''**. Keeping in mind that in these calculations the binding of alkenes to the Rh center is underestimated[8] (in part due to the fact that in these calculations attractive van der Waals interactions are underestimated), the overall energy barrier for propene (and ethane) insertion should in reality be substantially lower than +26.4 kcal mol^{-1}. The insertion of propene and rapid rearrangement of the conformation leads to the exothermic formation of the insertion product **D** (–9.5 kcal mol^{-1}), in which the polymer chain is located *cis* with respect to the allyl moiety of the cycloocta-2,5-dien-1-yl ligand. The optimized geometry of this structure **D** reveals a β-agostic interaction between the β-hydrogen of the growing alkyl chain and the metal (Figure S7) and the coordination of the ether is again restored.

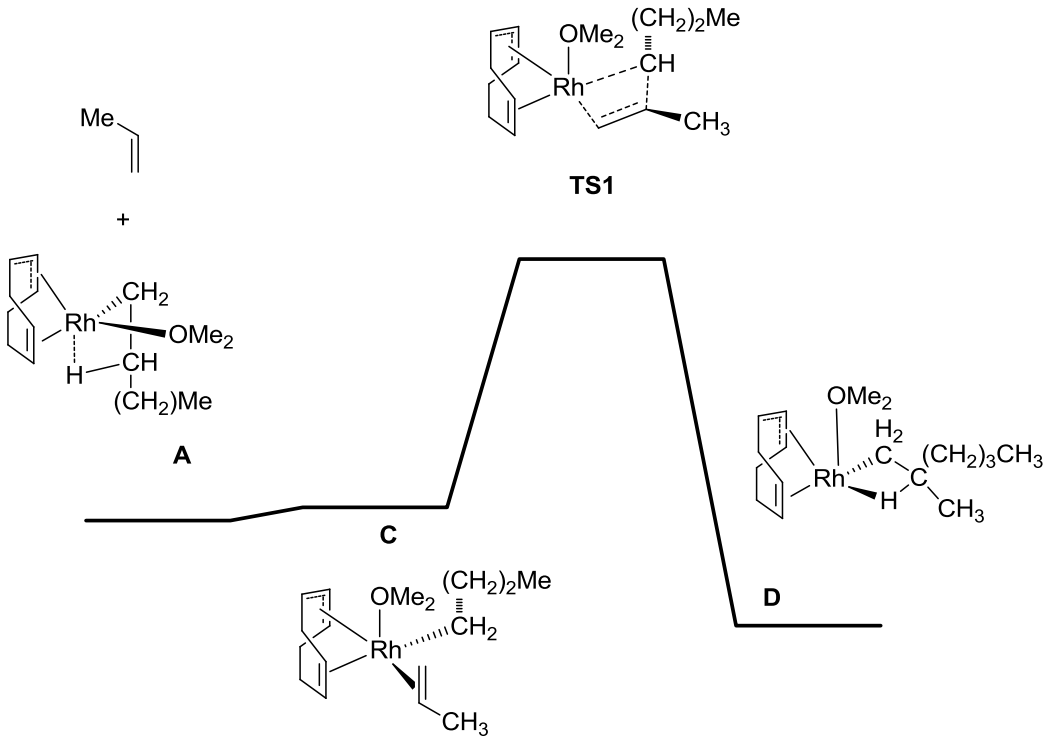

Figure S7. General representation of the calculated chain propagation pathway (b3-lyp, def2-TZVP) from complex **A** leading to branched polymers, involving propene insertion into the Rh–C bond of the growing chain.

Table S1. Calculated energies for propene insertion into the growing chain of species **A** (b3-lyp, def2-TZVP) in kcal mol^{-1} at 273 K.

Species	E_{scf}	E_{scf} + ZPE	ΔH^0	ΔG^0_{gas}	$\Delta G_{'solution'}$ [a]	$\Delta G_{'solution'}$ [b]
A	0	0	**0**	0	0	**0**
C	–1.4	+1.0	**+1.2**	+10.6	+8.1	**+4.4**
TS1	+22.1	+23.8	**+23.7**	+32.6	+30.1	**+26.4**
D	–12.2	–9.0	**–9.5**	+1.5	–1.0	**–4.7**

[a] Corrected for the condensed-phase reference volume (2.5 kcal mol^{-1} translational entropy correction).
[b] Entropy factors corrected towards 'solution phase' values using a Trouton-like approach (6.2 kcal mol^{-1} translational entropy correction).

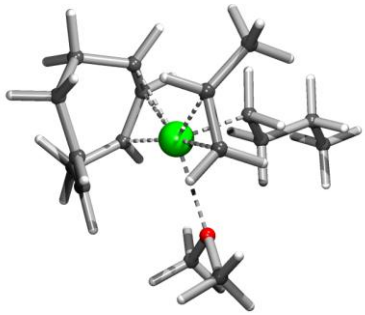

Figure S8. DFT-optimised geometry of propene-adduct **C**, showing the orientation of the propene fragment with respect to the cycloocta-2,5-dien-1-yl ligand.

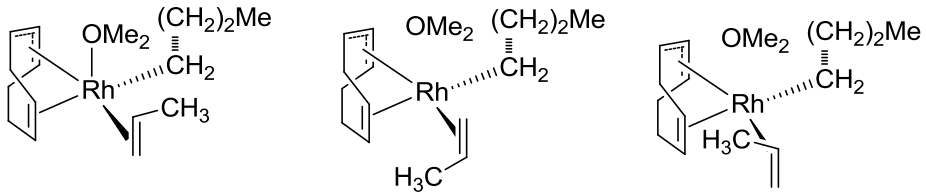

C' **C''** **C'''**

Figure S9. Representation of propene adducts **C'**, **C''** and **C'''**.

The pathway describing chain growth via ethene insertion into the alkyl chain is depicted in Figure S10 and Table S2. Coordination of ethene to species **A** is slightly exothermic and a geometry optimisation of this structure revealed that the ethene moiety adopts a parallel orientation with respect to the double bond of the cycloocta-2,5-dien-1-yl ligand. Insertion of ethene into the growing polymer chain occurs with a free-energy barrier (gas phase) of 27.1 kcal mol^{-1}. If we apply entropy corrections for the solvent phase, this barrier lowers to +20.9 kcal mol^{-1}. However, since the solubility of ethene gas in DCM or $CHCl_3$ is rather limited[9] it cannot be regarded as fully solvated and therefore by applying an entropy correction of 6.2 kcal mol^{-1} the energy barrier is underestimated. In reality, the value for the energy barrier will lie in-between the values for ΔG_{gas} and $\Delta G_{solution}{}^{b}$, and hence a more realistic estimate of the energy barrier for ethene insertion relative to 1-alkene (oligomer) insertion is obtained by taking the $\Delta G_{solution}{}^{a}$ value (i.e., +24.6 kcal mol^{-1}; in which the ΔG value is only corrected for the condensed-phase reference volume) for ethene to be compared with $\Delta G_{solution}{}^{b}$ for propene. As discussed above for propene and 1-alkenes, the energy barriers for alkene insertion are overestimated due to the fact that binding of alkenes (including ethene) to Rh is underestimated.[8] Therefore, the absolute energy barriers for propene and ethene insertion should in reality be substantially lower. The relative energy barriers for ethene and propene insertion obtained in the manner discussed above should however still be meaningful, and this provides a plausible explanation for the formation of alkyl branches in the copolymerization of EDA with ethane (see discussion below). Rapid rearrangement of the conformation leads to the formation of species **F** in an exothermic process (−16.0 kcal mol^{-1}). In this species **F** the growing polymer chain is located *cis* to the allyl fragment of the cycloocta-2,5-dien-1-yl ligand similar to starting complex **A** and as such, species **F** can easily enter a new catalytic cycle.

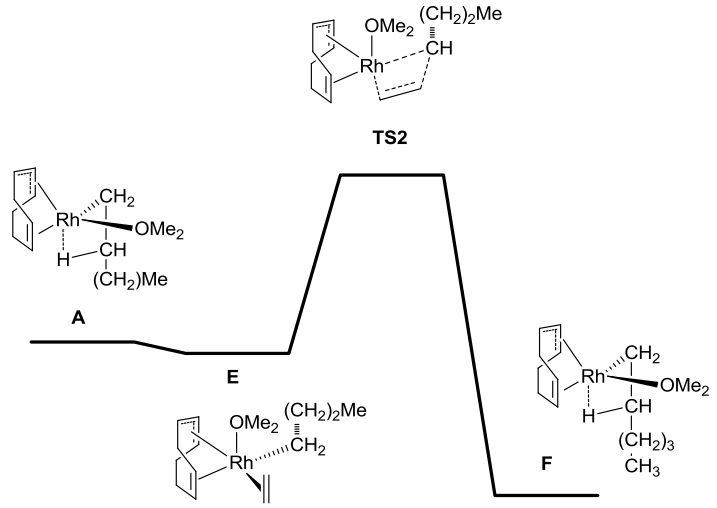

Figure S10. General representation of the calculated chain propagation pathway (b3-lyp, def2-TZVP) from complex **A** leading to linear polymers, involving ethene insertion into the Rh-C bond.

Table S2. Calculated energies for ethene insertion into the growing chain of species **A** (b3-lyp, def2-TZVP) in kcal mol^{-1} at 273 K.

Species	E_{scf}	E_{scf} + ZPE	ΔH^0	ΔG^0_{gas}	$\Delta G_{'solution'}$ [a]	$\Delta G_{'solution'}$ [b]
A	0	0	**0**	0	**0**	0
E	–4.1	+0.7	**–1.1**	+9.1	**+6.6**	+2.9
TS2	+15.8	+24.6	**+17.8**	+27.1	**+24.6**	+20.9
F	–19.0	–15.1	**–16.0**	–5.6	**–8.1**	–11.8

[a] Corrected for the condensed-phase reference volume (2.5 kcal mol^{-1} translational entropy correction).
[b] Corrected for the entropy using a Trouton-like approach (6.2 kcal mol^{-1} entropy correction).

The barrier for ethene insertion leading to linear polymers is very similar to that of the above-described insertion of a propene fragment, which would lead to branched polymers. This indicates that, taking into account the previously-described rather low barriers for β-hydride elimination and subsequent release of the alkene,[6] formation of branches via the pathway that involves insertion of such released 1-alkene fragments into the Rh–C bond of the growing polymer chain (see Figure S7) is feasible in the EDA-ethene copolymerisation reactions, which is in agreement with the observed experimental results. In fact, the chain propagation from branched species **D** should not be very different than from linear species **A**. The α-carbon of **D** is not branched and the branch at the β-carbon does not likely have a large steric influence on the subsequent carbene or ethene insertion steps. Hence, these computational models are in good agreement with the experimental results, and predict formation of branched polymers in case of (co)polymerisation with ethene. As described previously, for the linear copolymers of EDA and diazomethane the barrier for carbene insertion is much lower than that of propene insertion, and that explains why in that specific case we obtained linear copolymers. These computations therefore clearly explain the different behavior of ethene vs. diazomethane in copolymerisation reactions.

References in the Supporting Information

1 A. J. C. Walters, E. Jellema, M. Finger, P. Aarnoutse, J. M. M. Smits, J. N. H. Reek and B. de Bruin, *ACS Catalysis*, 2012, 2, 246.

2 M. P. Doyle, M. A. McKervey and T. Ye, *Modern Catalytic Methods for Organic Synthesis with Diazo Compounds*, John Wiley & Sons, New York, 2000.

3 H. Werner, P. Schwab, E. Bleuel, N. Mahr, P. Steinert and J. Wolf, *Chem. Eur. J.*, 1997, **3**, 1375.

4 T. Pechmann, C. D. Brandt and H. Werner, *Organometallics*, 2003, **22**, 3004.

5 N. M. G. Franssen, K. Remerie, T. Macko, J. N. H. Reek and B. de Bruin, *Macromolecules*, 2012¸ **45**, 3711.

6 N. M. G. Franssen, M. Finger, J. N. H. Reek and B. de Bruin, *Dalton Trans.*, accepted, DOI: 10.1039/C2DT32584E.

7 A. J. C. Walters, O. Troeppner, I. Ivanovic-Burmazovic, C. Tejel, M.P. del Río, J.N.H. Reek and B. de Bruin, *Angew. Chem. Int. Ed.* 2012, **51**, 5157.

8 S. Thewissen, Reactivity in the Gas Phase and Solution of Group 9 Metal Olefin Complexes (PhD Thesis), 2005, Appendix A.

9 B. I. Konobeev, V. V. Lyapin, *Khim. Prom.* 1967, **43**, 114-116.